J. Eng. Technol. Sci., Vol. 53, No. 2, 2021, 210212

Experiment-based Comparative Analysis of Nonlinear Speed Control Methods for Induction Motors

Vo Thanh Ha[1], Nguyen Tung Lam[2], Pham Van Tuan[3] & Nguyen Hong Quang[4],*

[1]University of Transport and Communications, Cau Giay Street, Lang Thuong Ward, Dong Da District, Hanoi 100000, Vietnam
[2]Hanoi University of Science and Technology, Dai Co Viet Road, Hai Ba District, Hanoi 100000, Vietnam
[3]Vinh University of Technology Education, Nguyen Viet Xuan Street, Vinh City 890000, Vietnam
[4]Thai Nguyen University of Technology, 3/2 Street, Thai Nguyen City 251750, Vietnam
*E-mail: quang.nguyenhong@tnut.edu.vn

Highlights:

- Presentation of design steps for speed and flux controllers based on backstepping, flatness-based control, and exact feedback linearization with state derivative for induction motor drives.
- A comprehensive comparison between nonlinear control structure responses.
- The research results are supported experimentally by practical simulation scenarios.

Abstract. Field-oriented control (FOC) for induction motors is widely used in industrial applications. By using a fast and accurate torque controller based on a stator current controller it is possible to flexibly implement advanced speed control methods to achieve proper performance both in transient and steady-state states. In this study, a deadbeat controller was used for the current loop. The nonlinear methods used for the outer loop controller were backstepping, flatness-based control, and exact feedback linearization with state derivative. The dynamic responses of these three controls were compared through various experimental results. The advantages and disadvantages of the different control structures were analyzed and evaluated in detail. Based on this evaluation, an appropriate scheme can be specified when deployed in practice.

Keywords: *backstepping; deadbeat control; exact linearization; flatness-based control; field oriented control; induction motor; PI.*

1 Introduction

Field-oriented control renders an induction motor (IM) as a separately excited DC motor with the same physical properties (magnetic flux forming and rotation torque producing) [1-4]. In the FOC structure, if the stator current controller is well-designed, the IM is considered as being fed by a current source inverter with

Received March 18th, 2020, Revised November 10th, 2020, Accepted for publication December 10th, 2020.
 ISSN: 2337-5779,
DOI: 10.5614/j.eng.technol.sci.2021.53.2.12

a controllable stator current, leading to model reduction of the IM from fourth-order to second-order. In the induction motor control structure, stator current i_{sd} is in charge of the magnetic flux forming and i_{sq} is the control input for the torque production. The induction motor dynamics also show bilinear nonlinearity because there is a multiplication component of i_m and i_{sq} [1-5]. Therefore, due to the important role of the stator current, it is necessary to have a control method such that the actual stator current closely tracks the reference current. A deadbeat current loop controller ensures the main target of the stator current, which is fast-accurate-decoupling compared to other control methods, such as PI control and exact linearization [5-8]. The design of the induction motor drive system according to an order-reduction model can be implemented in various ways. It has been shown that when operating in a wide range, the performance of the system degrades with the use of PI control [9-11]. Along with the strong development of hardware, nonlinear controllers [12,13] have been applied successfully in electrical drive systems.

This paper presents a comparative analysis of three nonlinear methods for speed and magnetic flux controls based on an order-reduction model of an induction motor. Firstly, we used a flatness-based control by selecting proper system outputs. Because of the order reduction of the differential equations it is relatively easy to set the trajectory of speed and magnetic flux only in the form of a second-order system with the time constant chosen from the current initial conditions [13-15,17-20]. Secondly, a control design was developed using backstepping control [16,21-23]. Finally, exact feedback linearization with state derivative was employed, where the nonlinear controller performs on the coordinate dq, which requires parameter estimation, and R_r, R_s are the rotor and stator resistances; L_s, L_r are the stator and rotor self-inductances; L_m is the stator-rotor mutual inductance; J is the inertia moment, and the derivative of the rotor flux angle and the rotor flux amplitude. The exact linearization control method combined with state derivative feedback overcomes heavy dependence on the state model parameters and signal measurement errors. However, the effectiveness of this nonlinear control method depends on accuracy of the state feedback signals [20-22] and [24-25]. The control methods were analyzed based on criteria for evaluating the quality of electric drives, i.e. torque ripple, speed overshoot and setting time, and robustness [12-14], which were verified via a set of experiments.

This paper organized as follows. The mathematical model of the IM is briefly given in Section 2. The control designs are presented in Section 3. Section 4 is dedicated to the experimental results. Finally, some important remarks are stated in Section 5.

2 Mathematical Model of the IM in *dq*-Coordinate

Consider the mathematical model of the induction motor on the *dq*-coordinate given as follows:

$$\begin{cases} \dfrac{di_{sd}}{dt} = -\left(\dfrac{1}{\sigma T_s} + \dfrac{1-\sigma}{\sigma T_r}\right) i_{sd} + \omega_s i_{sq} + \dfrac{1-\sigma}{\sigma T_r} + \dfrac{1}{\sigma L_s} u_{sd} \\ \dfrac{di_{sq}}{dt} = -\omega_s i_{sd} - \left(\dfrac{1}{\sigma T_s} + \dfrac{1-\sigma}{\sigma T_r}\right) i_{sq} - \dfrac{1-\sigma}{\sigma} \omega i_m + \dfrac{1}{\sigma L_s} u_{sq} \\ \dfrac{d\psi_{rd}}{dt} = -\dfrac{1}{T_r} \psi_{rd} + \dfrac{L_m}{T_r} i_{sd} \\ \dfrac{d\omega}{dt} = k_\omega \psi_{rd} i_{sq} - \dfrac{z_p}{J} m_L \end{cases} \tag{1}$$

where $\begin{cases} \omega_s = \omega_r + \omega; \omega_r = \dfrac{L_m}{T_r} \dfrac{i_{sq}}{\psi_{rd}}; \omega_s = \dfrac{L_m}{T_r} \dfrac{i_{sq}}{\psi_{rd}} + \omega \\ m_M = \dfrac{3}{2} z_p \dfrac{L_m}{L_r} \psi_{rd} i_{sq} \end{cases}$

It is clear that the IM is of the fourth order and comprises an electrical-magnetic-mechanical process. The motion of the IM in Eq. (1) is characterized by torque production, which is the scalar product of magnetic flux ψ_{rd} (created by *d*-component current i_{sq} -Isd) and *d*-component current i_{sq}. If the stator current controller satisfies the speed, accuracy and decoupling requirements, the motor model is reduced from the fourth-order Eq. (1). to the second-order Eq. (2), resulting in model reduction, including the magnetization and motion equations.

$$\begin{cases} \dfrac{di_m}{dt} = -\dfrac{1}{T_r} i_m + \dfrac{1}{T_r} i_{sd} \\ \dfrac{d\omega}{dt} = k i_m i_{sq} - \dfrac{z_p}{J} m_L \end{cases} \tag{2}$$

where: $i_m = \dfrac{\psi_{rd}}{L_m}; k = \dfrac{3}{2} \dfrac{z_p^2 L_m^2}{L_r J}$

3 Design of Nonlinear Outer Loop Controllers

With the use of a deadbeat controller it can be assumed that the stator current control is well-designed so in this study we could omit the current dynamics [12]. Therefore, the main objective of this study was to focus on evaluating the motor control structures for the outer control loop of the IM drives by looking at different possibilities of applying nonlinear control methods, such as flatness-based control, backstepping, exact linearization, and derivative state feedback.

3.1 Flatness-based Controller

Figure 1 shows that the flat output is magnetic flux and speed $\left[\psi_r'^d, \omega^d\right]$, the trajectory planning gives the reference values for flux and speed through the calculation of the reference inputs for the inner current loop. The magnetic flux trajectory design $\psi_{rd}'^{*}$ & $\psi_{rd}'^{d}$ can be given in the form of the following second-order system:

$$G_1 = \frac{\psi_{rd}'^{*}(s)}{\psi_{rd}'^{d}(s)} = \frac{1}{1 + T_1 s + T_1^2 s^2} \tag{3}$$

Rewriting Eq. (3) as a function of time gives:

$$\frac{d^2\psi_{rd}'^{*}}{dt^2} = \frac{1}{T_1^2}\left(\psi_{rd}'(t) - T_1\frac{d\psi_{rd}'^{*}}{dt} - \psi_{rd}'^{*}(t)\right) \tag{4}$$

In the same fashion, the magnetic flux trajectory is given as:

$$G_2 = \frac{\omega^*(s)}{\omega(s)} = \frac{1}{1 + T_2 s + T_2^2 s^2} \tag{5}$$

***Design of the feedforward controller*:**

In this flatness-based system, the input $\mathrm{u_T} = \left[i^*_{sd}; i^*_{sq}\right]$ is calculated based on the flatness output and construction trajectories as:

$$i^*_{sd} = \psi_{rd}'^{*} + T_r\frac{d\psi_{rd}'^{*}}{dt}; i^*_{sq} = \frac{h_1\dfrac{d\omega^*}{dt} + \tilde{m}_L}{h_2\psi_{rd}'^{*}} \tag{6}$$

where $\tilde{m}_L$ is the motor load, calculated by estimating the load; $h_1 = \dfrac{J}{z_p}; h_2 = T_r\dfrac{3}{2}z_p(1-\sigma)\dfrac{L_s}{L_m}\psi_{rd}^{*2}$ are the parameters.

Design of the feedback controller:

In fact, the derived state-space model of the induction motor is not absolutely accurate. In the model, all types of disturbances are ignored, so when using only feedforward control action, the resulting closed system output will have a steady-state error. Therefore, in order to ensure the tracking performance, a closed-loop control is required using the PI controller. The PI control structure of magnetic flux is:

$$R_{\psi}(z) = V_{\psi}\frac{1 - d_{\psi}.z^{-1}}{1 - z^{-1}} \tag{7}$$

The discrete PI speed control structure is:

$$G_r\left(z^{-1}\right) = \frac{V_R\left(1 + d_1.z^{-1}\right)}{\left(1 - z^{-1}\right)} \tag{8}$$

where V_{ψ}, V_R are amplification coefficients; $d_{\psi} = d_1 = a_1$ are standard convention parameters.

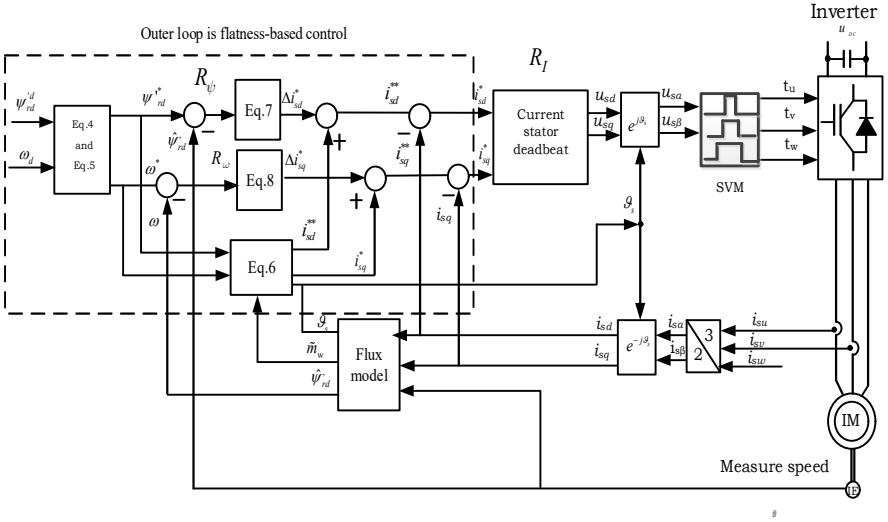

Figure 1 Induction motor drive with flatness-based control outer loop.

3.2 Backstepping Control Design

From Eq. (2), define the current error as:

$$z_1 = i_m - i_m^{*} \tag{9}$$

Taking the time derivative of Eq. (9) gives:

$$\dot{z}_1 = \frac{di_m}{dt} - \frac{di^*_m}{dt} = -\frac{1}{T_r} i_m + \frac{1}{T_r} i_{sd} - \frac{di^*_m}{dt} \tag{10}$$

We select the following Lyapunov candidate function:

$$V(z_1) = \frac{1}{2} z_1^2 \geq 0 \tag{11}$$

Then it can be shown that:

$$\dot{V}(z_1) = z_1 \dot{z}_1 = z_1 (-\frac{1}{T_r} i_m + \frac{1}{T_r} i_{sd} - \frac{di^*_m}{dt}) \tag{12}$$

To satisfy the Lyapunov stability:

$$\dot{V}(z_1) = -c_1 \dot{z}_1 \leq 0 \forall z_1 \quad (c_1 \text{ a constant positive number}) \tag{13}$$

Substituting Eq. (13) into Eq. (12) yields:

$$i_{sd} = -c_1 T_r z_1 + i_m + T_r \frac{di^*_m}{dt} \tag{14}$$

Design the backstepping control for the speed control loop:

From Eq. (2), define the speed error as:

$$z_2 = \omega - \omega^* \tag{15}$$

The time derivative of Eq. (15) is expressed as:

$$\dot{z}_2 = \frac{d\omega}{dt} - \frac{d\omega^*}{dt} = -\frac{z_p}{J} m_M + k i_{sq} - \frac{d\omega^*}{dt} \tag{16}$$

where $k = k_\omega i_m$. Choose Lyapunov candidate function V(z_2):

$$V(z_2) = \frac{1}{2} z_2^2 \geq 0 \tag{17}$$

Taking the time derivative of Eq. (18) :

$$\dot{V}(z_2) = z_2 \dot{z}_2 = z_2 (-\frac{z_p}{J} m_M + k i_{sq} - \frac{d\omega^*}{dt}) \tag{18}$$

To satisfy the Lyapunov criteria then:

$$\dot{V}(z_2) = -c_2 \dot{z}_2 \leq 0 \forall z_2 \, (c_2 \text{ is a constant positive number}) \tag{19}$$

Substituting Eq. (18) into Eq. (19) results in:

$$i_{sq} = \frac{1}{k}(-c_2 z_2 + \frac{z_p}{J} m_M + \frac{d\omega^*}{dt}) \tag{20}$$

It should be noted that due to the assumption of ideal current control, Eq. (14) and Eq. (21) indicate the current control outputs. The induction motor control scheme based on backstepping is shown in Figure 2.

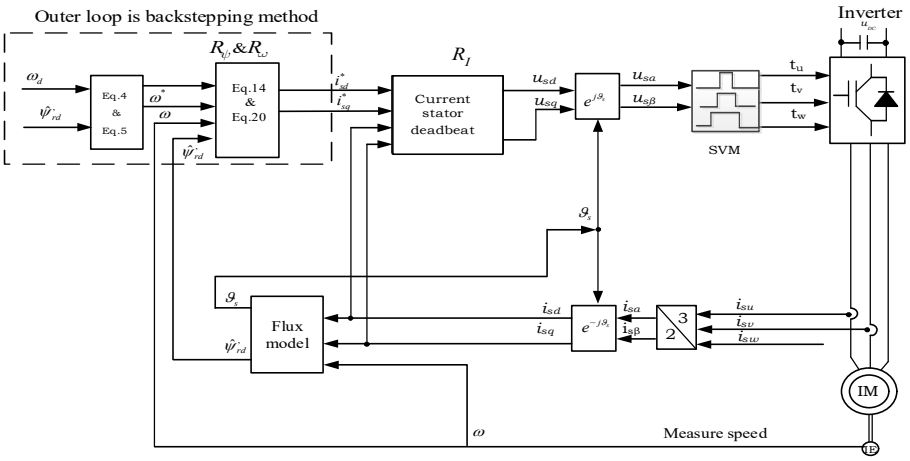

Figure 2 Induction motor drive with backstepping-based control outer loop.

3.3 Exact Linearization with State Derivative Feedback

Exact linearization with state derivative feedback was done through the design of a speed and magnetic flux controller based on nonlinear control methods such as flatness-based control and backstepping in Section 3.1 and 3.2. It is noted that these control strategies are based on speed and flux information that is sensitive to the induction motor parameters. For example, rotor resistance R_r, stator R_s, inductance L_m vary when the IM operates over a considerable period of time.

In practice there is always a deviation between the calculated and the actual values of the parameters. In addition, they also depend on the load torque, the moment of inertia, and coefficients of the mechanical structure connecting the motor such as damping coefficient d and shaft-stiffness c [12] and [13]. This affects the stability and control quality of the IM drive system. With the application of a deadbeat current control [5] and the assumption of an ideal current response, the IM model can be represented as:

$$\begin{cases} \dfrac{d\psi_{rd}}{dt} = a\psi_{rd} + aL_m i_{sd} \\ \dfrac{d\theta_{rf}}{dt} = z_p\omega + \dfrac{a}{\psi_{rd}} L_m i_{sq} \\ \dfrac{d\omega}{dt} = \dfrac{3}{2} z_p \dfrac{L_m}{JT_r} \psi_{rd} i_{sq} - \dfrac{z_p}{J} m_L - \dfrac{d}{J}\omega \end{cases} \tag{21}$$

where: $a = R_r / L_r$; θ_{rf} is the rotor flux angle; d is the friction coefficient. It is noted that the control model Eq. (21) is of the third order, where the first equation gives the magnetic flux, the second equation gives the rotor flux rotation, and the third equation gives the rotational motion. The second equation, which is the dynamic state variable measured in terms of participating in the design of the speed and flux controller for a squirrel cage rotor according to the method of exact linearization with derivative-state feedback. The control model is divided into two subsystems. The first subsystem consists of the magnetic flux equation and the rotor flux rotation angle while the second subsystem consists of the rotating motion equation characterized by uncertainty parameters such as friction stiffness d, moment of inertia J, load moment m_L. The first subsystem was applied to the design of the speed and magnetic flux controllers, because this subsystem is less dependent on the motor parameters, link structure, torque, etc.

From the mathematical equation of the induction motor [1], a subsystem was designed for the speed and magnetic flux controller according to the method of exact linearization with derivative state feedback:

$$\begin{cases} \dfrac{d\psi_{rd}}{dt} = a\psi_{rd} + aL_m i_{sd} \\ \dfrac{d\theta_{rf}}{dt} = z_p\omega + \dfrac{aL_m i_{sq}}{\psi_{rd}} \end{cases} \tag{22}$$

With state variable: $x_1 = \psi_{rd}; x_2 = \theta_{rf}$; input variable: $u_1 = i^*_{sd}; u_2 = i^*_{sq}$. Eq. (22) can be described by the following affine nonlinear equation system:

$$\begin{cases} \dfrac{d\mathbf{x}}{dt} = \mathbf{f(x)} + \mathbf{H(x)u} \\ \mathbf{y} = \mathbf{g(x)} \end{cases} \tag{23}$$

where:

$$x = \begin{bmatrix} \psi_{rd} \\ \theta_{rf} \end{bmatrix}; f(x) = \begin{bmatrix} -a\psi_{rd} \\ z_p\omega \end{bmatrix}; H(x) = \begin{bmatrix} aL_m & 0 \\ 0 & (aL_m)/\psi_{rd} \end{bmatrix}$$

Eq.(23) can be expressed as:

$$\begin{cases} \dfrac{dx_1}{dt} = -a\psi_{rd} + aL_m i_{sd} \\ \dfrac{dx_2}{dt} = z_p \omega + aL_m i_{sq} / \psi_{rd} \end{cases} \tag{24}$$

It is noted that in the system of Eq. (24) the output vector contains input vector ***u*** ($u_1 = i^*_{sd}; u_2 = i^*_{sq}$) and the system of Eq. (24) can be exactly linearized. Therefore, we have an input vector ***u*** of the following form:

$$\mathbf{u} = \mathbf{H}^{-1}(\mathbf{x})[\dot{\mathbf{x}} - \mathbf{f}(\mathbf{x})] \tag{25}$$

Deriving an optimal control algorithm that separates the input and output vectors is done as follows:

$$\mathbf{y}(t) = \mathbf{u}^*(t) \tag{26}$$

Eq. (25) can be rewritten:

$$\mathbf{u} = \mathbf{H}^{-1}(\mathbf{x})[\dot{\mathbf{x}} - \mathbf{f}(\mathbf{x}) + (\mathbf{u}^* - \mathbf{g}(\mathbf{x}))] \tag{27}$$

Expressed in Eq. (27):

$$i_{sd} = \frac{1}{aL_m}\left[(\frac{d\psi_{rd}}{dt} + a\psi_{rd}) + (\psi^*_{rd} - \psi_{rd}) \right] \tag{28}$$

$$i_{sq} = \frac{\psi_{rd}}{aL_m}\left[(\frac{d\theta_{rf}}{dt} - z_p\omega) + (\omega^* - \omega) \right] \tag{29}$$

From Eq. (28) and Eq. (29) it is realized that these are the two equations used to calculate the speed and magnetic flux values as required. Substituting Eq. (28) and Eq. (29) into Eq. (22) we get:

$$\begin{cases} \psi_{rd} = \psi^*_{rd} \\ \omega = \omega^* \\ \dfrac{d\theta_{rf}}{dt} = z_p\omega^* + \dfrac{aL_m}{b\psi^*_{rd}}\left[\dfrac{d\omega^*}{dt} + (\dfrac{d}{J})\omega^* + (\dfrac{1}{J})m_L \right] \end{cases} \tag{30}$$

It can be seen from the system of Eq. (30) that the actual signals of speed and magnetic flux are equal to the reference signals and that the error is zero. To implement the design of the speed controller in Eq. (30) and the magnetic flux controller in Eq. (30), an estimator must be developed to calculate the parameters,

the derivative of the rotor flux and the rotational magnetic flux of the rotor. The PD controller was used here, because it is simple and efficient to implement. The estimated value is calculated by Eq. (31).

$$\frac{d}{dt}\begin{bmatrix}\hat{\psi}_{rd}\\ \hat{\theta}_{rf}\end{bmatrix}=\begin{bmatrix}-a\hat{\psi}_{rd}+aL_m i_{sd}\\ z_p\omega+(aL_m i_{sq})/\hat{\psi}_{rd}\end{bmatrix} \tag{31}$$

Thus, fast and accurate current control is performed by the deadbeat controller, we have a speed and magnetic control structure designed by the method of exact linearization combined with derivative state feedback, as shown in Figure 3.

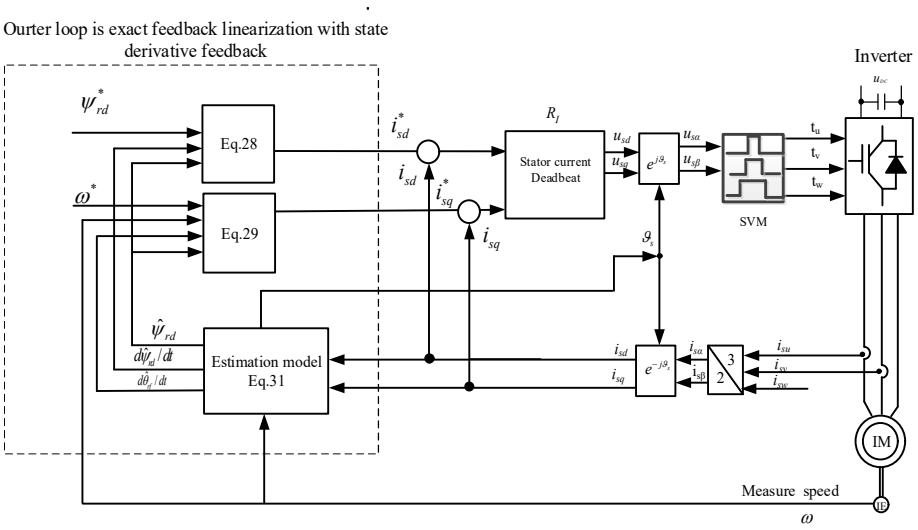

Figure 3 The structure for an asynchronous motor with an inner loop as a dead-beat controller; the outer loop is the exact linearization with derivative state feedback controller.

The control structure in Figure 3 shows that the speed and magnetic flux controller are omitted, where the reference stator current i_{sd}^*, i_{sq}^* is calculated directly through the rotor flux state and the rotor flux rotation with the condition that the real signal is identical to the reference signal. This is one of the advantages of the controller, which allows the induction motor to operate in the full speed range, with any torque, inertia torque (within the operating limits of the motor).

The controllers Eqs. (28) and (29) only need to know the rotor time constant, inductance, number of pairs of poles, measured by the estimator in Eq. (31). Thus, it is recognized that this control method uses a minimum number of IM parameters, so it is necessary to use an estimator in the control structure, which is also the current research trend. In addition, the estimator in Eq. (31) improves the system's robustness significantly, whether there are deviations or not, guaranteeing the exact motor parameters between the calculation theory and reality.

4 Experimental Results

Electric drive performance indicators such as torque response in no-load and loaded conditions are considered in this section. In addition, the quality of the electric drive is assessed through the speed of response in the transient state. The system's robustness is subsequently examined under variation of the motor parameters. Experiments were conducted on an induction machine with the parameters given in Table 1. The structure of the test bench is shown in Figure 4.

Table 1 Experimental parameters.

Motor parameter	Notation
Rated power	$P_N = 2.2$ kW
Rated current	$I_N = 4.7$ A
Rated frequency	$f_N = 50$ Hz
Power factor	$\cos\varphi = 0.8$
Number of pairs of poles	$z_p = 1$
Rated speed	$n_N = 2880$ round/minute
Rated voltage	$U_N = 400$ V
Stator resistor	$Rs = 0.37\ \Omega$
Rotor resistor	$Rr = 1.99\ \Omega$
Stator inductance	$L_s = 0.03441$ H
Stator inductance	$L_r = 0.03425$ H
Coefficient of mutual inductance between rotor and stator	$L_m = 0.0331$ H

First we see how the motor speed control loop reacts by operating the motor in a speed range from 100 rad/s (100 rpm) to 0.1 rad/s (1 rpm), especially at low speed (where low inertia makes it hard for the drive to operate properly). The experiment was carried out with no-load and a constant torque of 1.5 (N.m); the motor parameters are given in Table 1.

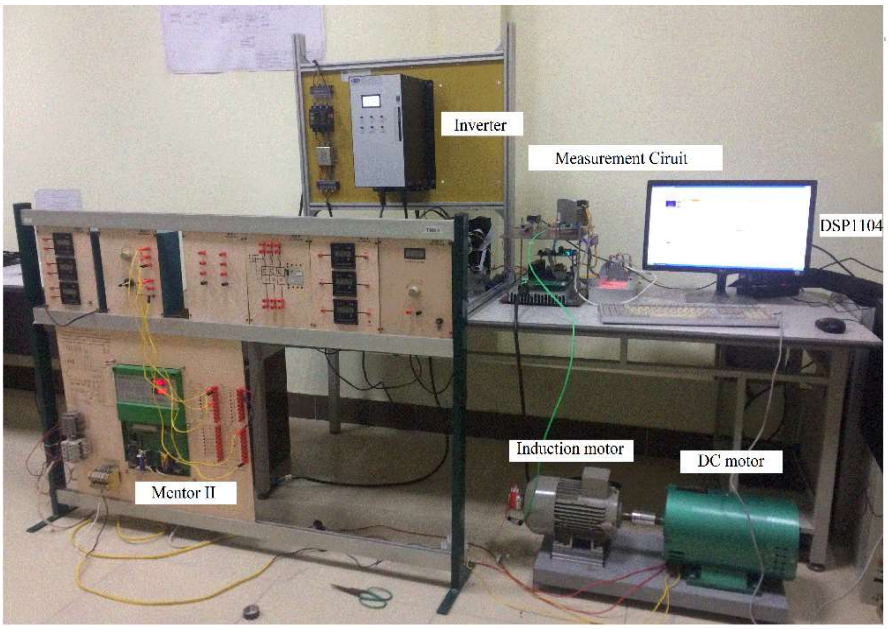

Figure 4 Experimental setup.

The experimental results are shown in Figure 5, Figure 6 and Table 2. Through the experimental setup depicted in Figure 5 and Table 2, it can be concluded that the above control structures performed well with a short settling time, from 0.15 s to 0.25 s, and a small overshoot of 4%. The recorded pulse rate torque ranged from $Rm_F\%$ 2.0% to 4.2%, while the maximum pulse rate torque $\Delta m_M\%$ was 4% when the motor speed was 100 rad/s.

At a speed of 0.1 rad/s, the pulse rate torque $\Delta m_M\%$ was very high. However, the control structure with the deadbeat inner and outer loop using the exact linearization method with the derivative state feedback gave better results in comparison with the other two control structures.

The robustness of the electric drive was validated by changing (increasing) the rotor resistance. This parameter is directly related to the dynamical response of the IM as the value of R_r increases, affecting the rotor time constant $T_r = L_r / R_r$. In the experimental scenario we changed R_r linearly from the nominal value.

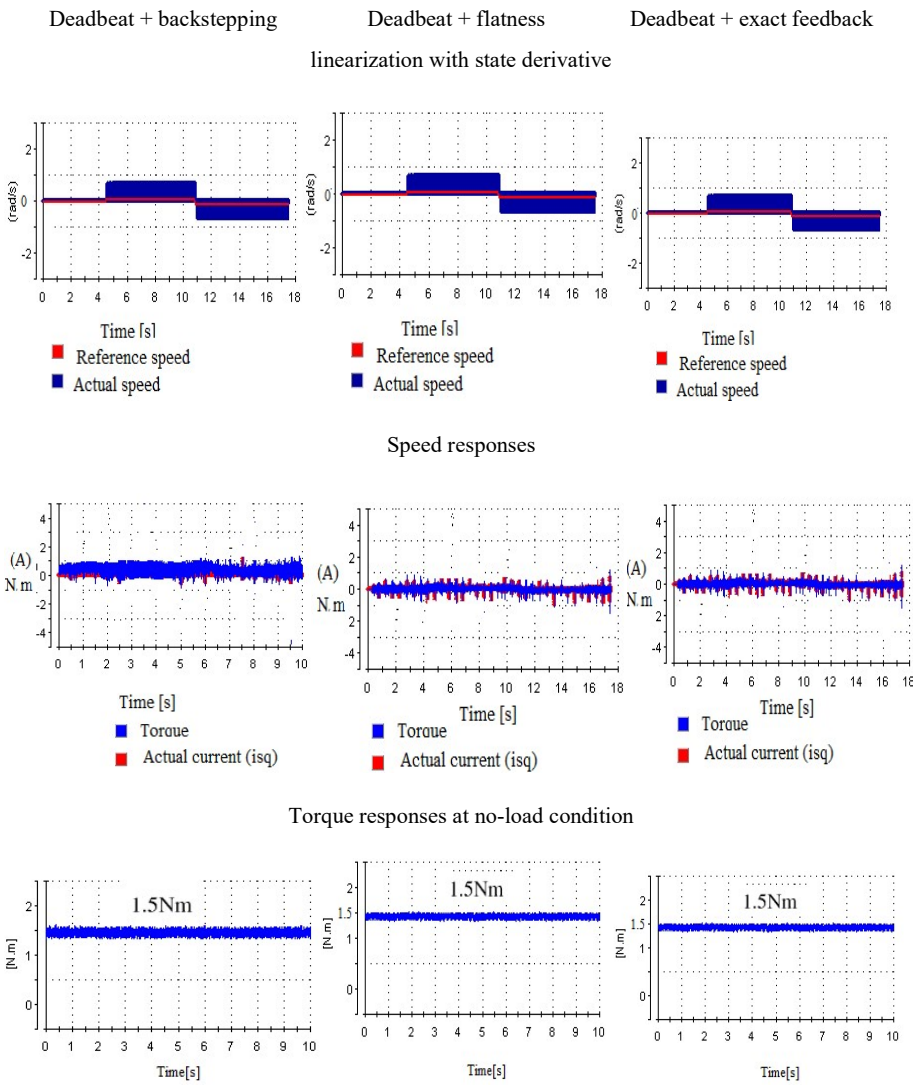

Figure 5 Speed and torque responses at a speed of 0.1 rad/s.

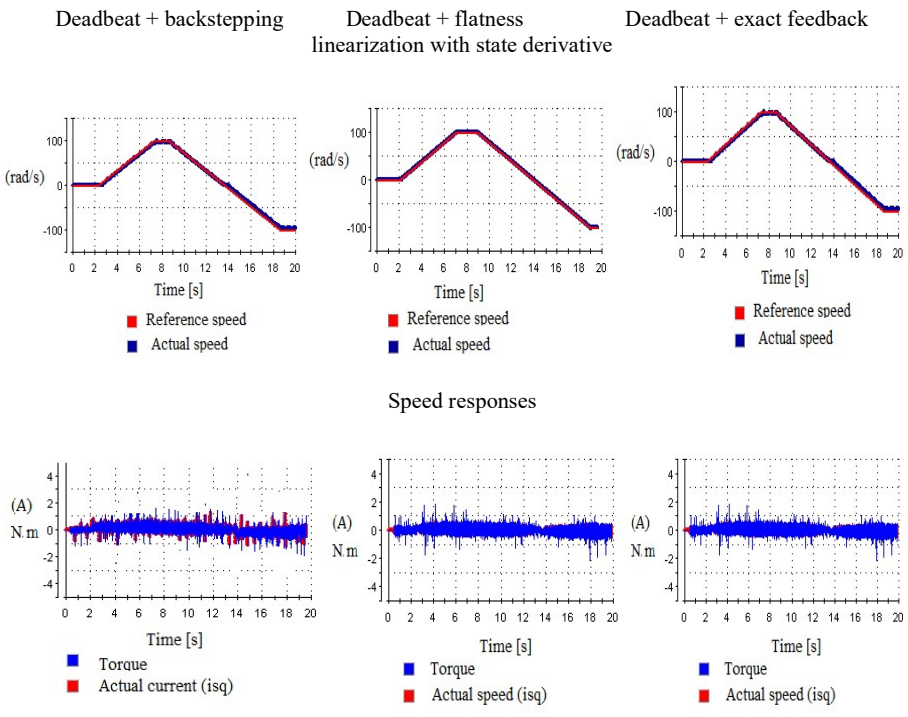

Figure 6 Speed and torque responses at a speed of 100 rad/s.

Table 2 Simulating results of evaluation and comparison of the quality of electric drive control structures.

FOC control structure	Deadbeat backstepping	Deadbeat flatness	Deadbeat exact feedback linearization with state derivative
Motor speed at 0.1 rad/s			
Settling time (s)	0.25	0.2	0.15
RT_F%	2.67	2.7	2.0
ΔT_m %	50	45	30
Motor speed at 100 rad/s			
Settling time (s)	0.25	0.2	0.15
RT_F%	4.0	4.2	3.0
ΔT_m %	10	8	4.0

Through the results in Figure 7, we look at Table 3 to assess the drop in the speed and torque responses when the rotor resistance R_r increases.

Through the experimental results presented in Figure 7 and Table 3 it can be seen that when the rotor resistance R_r increases, the torque amplitude increases gradually and the speed tracking error is not obvious. When the value was increased by 150% of the nominal value of R_r, degradation of the torque and the speed could be observed.

Compared to the other two schemes, the structure of a deadbeat current stator loop with a speed loop with exact linearization and derivative state feedback gave better system robustness against rotor resistance fluctuation.

Table 3 Assessing the drop of speed and torque when the rotor resistance rr increased.

Evaluation criteria	Deadbeat backstepping	Deadbeat flatness	Deadbeat + exact feedback linearization with state derivative
The ripper speed $\Delta\omega$ (%)	4.87	3.69	0.89
The ripper torque ΔT_m (%)	20	16	5

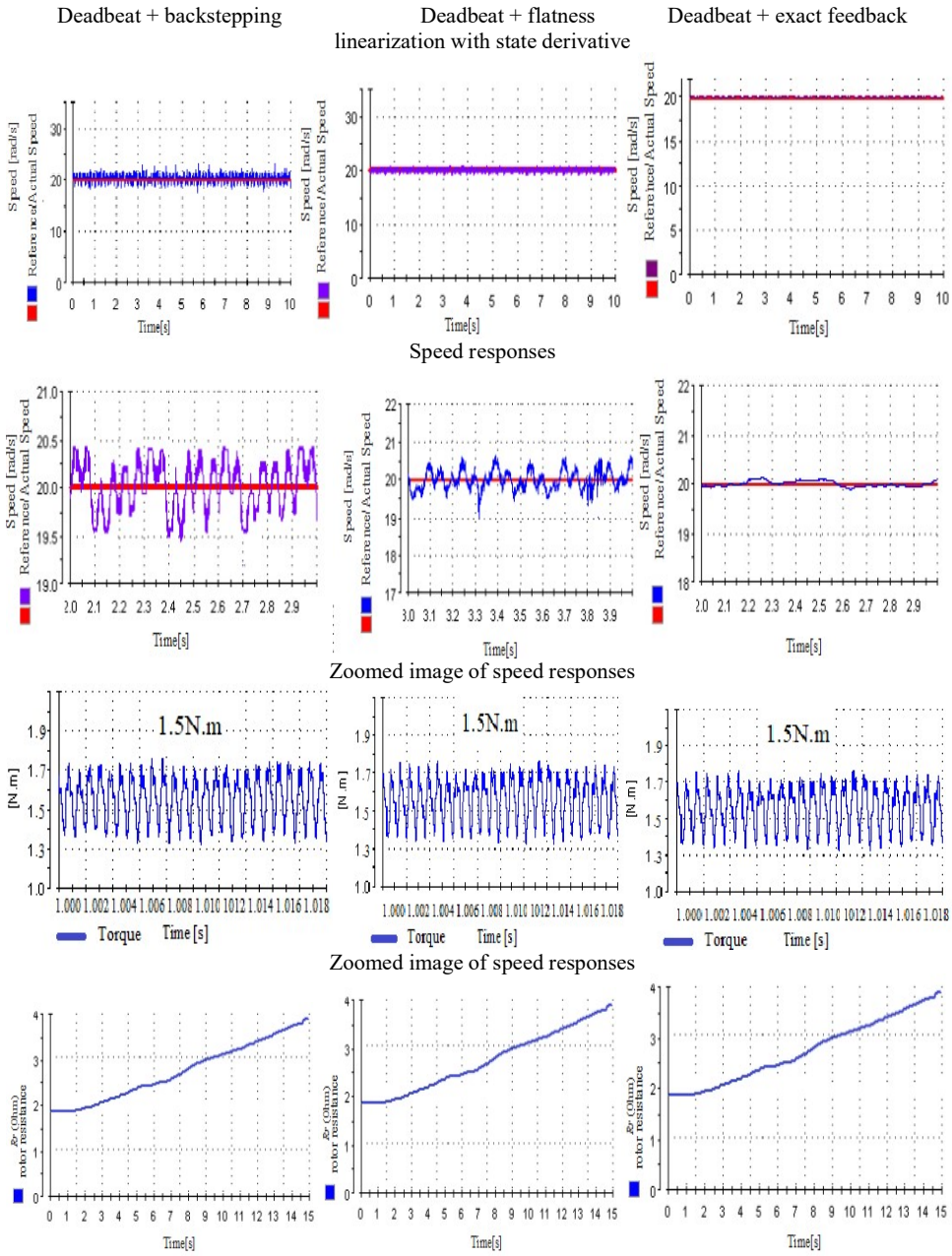

Figure 7 Speed response, torque response and value of rotor resistance R_r increasing to 50%.

5 Conclusion

It is indicated that with the assumption of an ideal current loop, different speed controls can be employed, namely flatness, backstepping, and exact linearization integrated with derivative state feedback. From the experimental studies it was found that exact linearization combined with derivative-state feedback for a speed and magnetic flux controller has the advantages of a simple design and speed tracking performance. In addition, this control method does not depend heavily on parameter changes. The results of this study suggest a way to design an outer controller for complex electric drive systems, such as two soft-coupling inertia, multi-mass systems, with the aim of improving the quality of the electric drive system. Future work will involve a comprehensive study of the abovementioned controls in relation to various common load characteristics.

Acknowledgement

This research was supported by the Research Foundation of Thai Nguyen University of Technology.

References

[1] Quang, N.P. & Dittrich J.A., *Vector Control of Three-phase AC Machines*, System Development in the Practice, 2nd edition, Springer-Verleg Berlin Heidelberg, 2015.

[2] Leonhard, W., *Control of Electrical Drives*. 3rd edition, Springer, 2001.

[3] Salo, M., & Tuusa, H., *Vector-Controlled PWM Current-Source-Inverter-Fed Induction Motor Drive with a New Stator Current Control Method*, in IEEE Transactions on Industrial Electronics, **52**(2), pp. 523-531, April 2005.

[4] Chiasson, J., *Modeling and High-Performance Control of Electrics Machines*, IEEE Series on Power Engineering, Wiley-IEEE Press, 2005.

[5] Quang, N.P., Ha, V.Y. & Trung, T.V., *A New Control Design with Dead-Beat Behavior for Stator Current Vector in Three-Phase AC Drives*, International Journal of Electrical and Electronics Engineering (SSRG-IJEEE), **5**(4), pp. 1-8, April 2018.

[6] Yang, S.M. & Lee, C.H., *A Deadbeat Current Controller for Field Oriented Induction Motor Drives*, IEEE Transactions on Power Electronics, **17**(5), pp. 772-778, October 2002.

[7] Neves, F., Menezes, B. & Silva, S., *A Stator Flux Oriented Induction Motor Drive with Deadbeat Direct Torque and Flux Control*, Electr Power Compon Syst, **32**(12), pp. 1319-1330, 2004.

[8] Kenny, B. & Lorenz, R., *Stator and Rotor Flux-based Deadbeat Direct Torque Control of Induction Machines*, IEEE Trans Ind Appl, **39**(4), pp. 1093-1101, 2003.

[9] Wang, L., Chai, S., Yoo, D., Gan, L. & Ng, K., *PID and Predictive Control of Electrical Drives and Power*, Wiley-IEEE Press, ISBN: 978-1-118-33944-2, Mar 2015.

[10] Szabat, K. & Orlowska-Kowalska, T., *Vibration Suppression in a Two-mass Drive System Using PI Speed Controller and Additional Feedbacks – Comparative Study*, Ind. Electronic. IEEE Transactions on Industrial Electronics, **54**(2), pp. 1193-1206, April 2007.

[11] Han, J., *From PID to Active Disturbance Rejection Control*, IEEE Transactions on Industrial Electronics, **56**(3), pp. 900-906, March 2009.

[12] Ha, V.T., Lam, N.T., Ha, V.T. & Vinh, V.Q., *Advanced control structures for Induction Motors with Ideal Current Loop Response Using Field Oriented Control*, Int. J. Power Electron. Drive Syst., **10**(4), pp. 1758-1771, 2019.

[13] Ha, V.T., Tan, L.T., Nam, N.D. & Quang, N.P., *Backstepping Control of Two-mass System Using Induction Motor Drive Fed by Voltage Source Inverter with Ideal Control Performance of Stator Current*, International Journal of Power Electronics and Drive System (IJPEDS), **10**(2), pp. 720-730, 2019.

[14] Khalil, H., *Nonlinear Systems*, Pearson, 2002.

[15] De Doncker, R., Duco, W.J. Pulle, Veltman, A., *Advanced Electrical Drives: Analysis, Modeling, Control, Advanced Electrical Drives*, Springer, Dordrecht/Heidelberg/London/New York, 2011. DOI:10.1007/978-94-007-0181-6.

[16] Burns, R.S., *Advanced Control Engineering*, Butterworth-Heinemann November 21, 2001.

[17] Dannehl, J. & Fuchs, F.W., *Flatness-based Control of an Induction Machine Fed via Voltage Source Inverter – Concept,* Control Design and Performance Analysis, IECON 2006 – 32nd Annual Conference on IEEE Industrial Electronics, Paris, pp. 5125-5130, 2006.

[18] Thomsen, S. & Fuchs, F. W., *Flatness Based Speed Control of Drive Systems with Resonant Loads*, Proceedings of the 2011 14th European Conference on Power Electronics and Applications, Aug. 30 - Sept. 1, 2011.

[19] Berrezzek, F., Bourbia, W. & Bensaker, B., *Flatness Based Nonlinear Sensorless Control of Induction Motor Systems*, International Journal of Power Electronics and Drive System (IJPEDS), **7**(1), pp. 265-278, March 2016.

[20] Quang. N.H., *Flatness Based Control Structure for Polysolenoid Permanent Stimulation Linear Motors*, SSRG International Journal of Electrical and Electronics Engineering, **3**(12), pp. 31-37, 2016.

[21] Mola, M., Khayatian, A. & Dehghani, M., *Backstepping Position Control of Two-mass Systems with Unknown Backlash*, 9th Asian Control Conference (ASCC), Istanbul, pp. 1-6, 2013.

[22] Ameid, T., Menacer, A., Talhaoui, H., Harzelli, I. & Ammar, A., *Backstepping Control for Induction Motor Drive Using Reduced Model in Healthy State: Simulation and Experimental Study,* 6th International Conference on Systems and Control (ICSC), Batna, pp. 162-167, 2017.

[23] Trabelsi, R., Kheder, A., Mimouni, M.F. & M'sahli, F., *Backstepping Control for an Induction Motor with an Adaptive Backstepping Rotor Flux Observer,* 18th Mediterranean Conference on Control and Automation, MED'10, Marrakech, pp. 5-10, 2010.

[24] Nam, D.P., *Multi Parametric Programming and Exact Linearization based Model Predictive Control of a Permanent Magnet Linear Synchronous Motor*, International Conference on System Science and Engineering (ICSSE), pp. 743-747, 2017.

[25] Boukas, T.K., *T.G. Habetler Exact Feedback Linearization with State Derivative Feedback for High-performance Field-oriented Induction Motor Speed/Position Control,* 38th IAS Annual Meeting on Conference Record of the Industry Applications Conference, 2003.